A CONCEPTUAL WING FLUTTER ANALYSIS TOOL FOR SYSTEMS ANALYSIS AND PARAMETRIC DESIGN STUDY

Vivek Mukhopadhyay

NASA Langley Research Center,
Hampton, VA 23681, USA
e-mail: v.mukhopadhyay@larc.nasa.gov

Key words: Conceptual Flutter analysis, wing design parameters, Regier number, flutter number, bending, torsion, frequency, blended wing body.

Abstract: An interactive computer program was developed for wing flutter analysis in the conceptual design stage. The objective was to estimate flutter instability boundaries of a typical wing, when detailed structural and aerodynamic data are not available. Effects of change in key flutter parameters can also be estimated in order to guide the conceptual design. This user-friendly software was developed using MathCad and Matlab codes. The analysis method was based on non-dimensional parametric plots of two primary flutter parameters, namely Regier number and Flutter number, with normalization factors based on wing torsion stiffness, sweep, mass ratio, taper ratio, aspect ratio, center of gravity location and pitch-inertia radius of gyration. These parametric plots were compiled in a Chance-Vought Corporation report from database of past experiments and wind tunnel test results. An example was presented for conceptual flutter analysis of outer-wing of a Blended-Wing-Body aircraft.

1 INTRODUCTION

During conceptual design of a wing, it is often necessary to obtain initial estimates of the wing or tail flutter boundary, when only the basic plan-form is known, and much of the structural data, frequency, mass and inertia properties are yet to be established. It is also very useful to conduct a parametric study to determine the effect of change in Mach number, dynamic pressure, torsion frequency, wing sweep-back angle, mass ratio, aspect ratio, taper ratio, center of gravity, and pitch moment of inertia, on the flutter boundary. For this purpose, an interactive computer program was developed using MathCad[1] and Matlab application software, for rapid interactive empirical flutter analysis. This flutter analysis method was based on non-dimensional parametric plots of two primary flutter parameters, namely normalized Regier number and Flutter number versus Mach number. The normalization factors are based on wing geometry, torsion stiffness, sweep, mass ratio, taper ratio, aspect ratio, center of gravity position and pitch inertia radius of gyration. This empirical flutter analysis method and all parametric plots were originally developed by Harris[2] from large number of wind-tunnel flutter model test data reports. Regier number is a stiffness-altitude parameter, first studied by Regier[3] for scaled dynamic flutter models. Regier number was also used by Frueh[4] as a flutter design parameter. Dunn[5] used Regier number to impose flutter constraints on the structural design and optimization of an ideal wing. In this paper, general assumptions, data requirements and interactive analysis procedure are described. Important non-dimensional plots used for the analysis, and an example to estimate the flutter boundary and stiffness requirements of the outer wing of a blended wing-body concept[6] was presented. From a set of initial data, preliminary flutter boundary and flutter dynamic pressure variation with Mach number, and root-chord torsion stiffness were determined.

2 GENERAL ASSUMPTIONS

The flutter analysis software is applicable for a conventional cantilevered wing or tail with straight leading and trailing edge as shown in Fig. 1. The primary geometric input data required are root-chord CR, tip-chord CT, effective semi-span S, sweep at quarter chord Λ, chord-wise location of wing section center of gravity at 60% semi-span and location of elastic axis or hinge-line for all pitching surface at root chord. The lifting surface of the wing is assumed to be rigidly clamped at an effective root station, and has conventional bending-torsion type flutter characteristics. If this effective root is not clamped, a correction factor is applied to account for the effect of bending and torsion flexibility at this wing station. This feature is useful for an all moving tail surface mounted on a flexible rod or for a blended wing-body type structure where the outer span of the wing is more flexible and primarily contributes to flutter instability and the inner part is relatively rigid. Then the span-wise station of the flexible outer wing is used as effective root station and a correction factor is applied to account for the bending freedom.

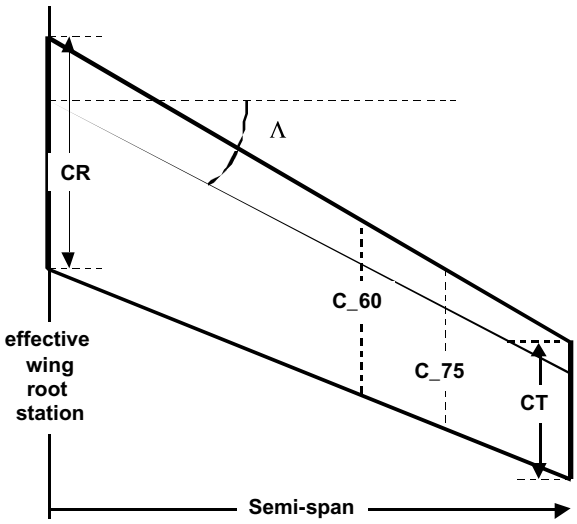

Fig. 1 Conventional wing planform geometry definition.

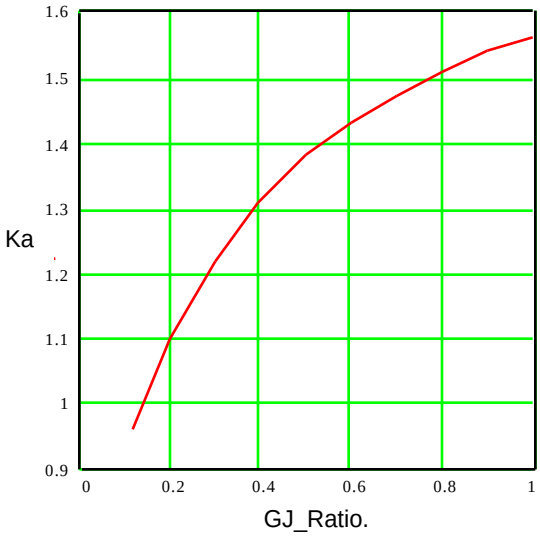

Fig. 2 Ka vs.GJ_Ratio plot for estimating ω_α.

The interactive analysis starts with specifying the geometric data and the critical design input parameters. These numerical data can be assigned or changed interactively on the computer screen, for all the parameters which are followed by the assignment symbol :=, and are marked as INPUT. At a later stage, for parametric study, a series of values can also be assigned directly. The rest of the analysis equations, related data and functions are automatically calculated, and all data are plotted to reflect the effect of the new input parameters. The units are also checked for compatibility and converted to the database units before calculations are performed. The primary input data required are root-chord CR, tip-chord CT, effective semi-span S, sweep at quarter chord Λ, running pitch moment of inertia I_60 and running weight W_60, both at 60% effective semi-span, chord-wise location of center of gravity line CGR at 60% semispan as fraction of mean geometric chord and total weight of the exposed surface W_ex. Structural data required are torsion stiffness at wing root GJ_root and at mid-span GJ_mid from which first torsion frequency ω_α is computed. If structural data are not available for computing the wing uncoupled

torsion frequency ω_α, an empirical formula[2] based on a torsion frequency factor Ka can be used, as shown in Eq. (1) in radians/second.

$$\omega_\alpha = \frac{Ka}{L}\sqrt{\frac{GJ\_root}{I\_60/g}} \tag{1}$$

Fig. 2 shows the plot of the factor Ka as a function of GJ_Ratio, which is defined as GJ_midwing/GJ_root. Using the computed GJ_Ratio, the factor Ka is obtained from Fig. 2 using a linear interpolation, and the torsion frequency ω_α is computed from Eq. (1). Alternatively, primary bending and torsion natural frequencies may be supplied. A typical interactive data input screen is shown in Fig. 3. Location of elastic axis (or hinge-line for all moving surface) and the ratio of primary torsion over bending frequency are also required as input. The input for reference flutter critical flight altitude and Mach number are generally chosen at sea level and at maximum design dive speed, respectively. This basic input is used to compute two basic flutter indexes, namely Regier number and Flutter number, and are described next.

4 REGIER NUMBER AND FLUTTER NUMBER

The first important non-dimensional parameter called surface Regier number R and the surface Regier velocity index V_R are defined at sea level by Eqs. (2, 3).

$$\text{Regier\_no}\quad R = V\_R/a_0 = \frac{0.5C_{75}\omega_\alpha\sqrt{\mu_0}}{a\sqrt{\sigma}} \tag{2}$$

where Regier surface (sea level) velocity index V_R is defined as

$$V\_R = 0.5C_{75}\omega_\alpha\sqrt{\mu_0} \tag{3}$$

The surface (sea level) Regier number can be interpreted as a ratio of elastic force over aerodynamic force at sea level. The Regier surface velocity index V_R (called surface flutter parameter in Ref. 2) is proportional to uncoupled torsion frequency ω_α, and has the unit of velocity. V_R is defined as a parametric function denoted by V_R(GJ_Ratio, GJ_root, I_60, L, C_75, μ0). Here, mass ratio $\mu 0 := W\_ex/[\pi.\rho 0.\int_0^s (c/2)^2 dy]$. The second important non-dimensional parameter called Flutter number F is defined as equivalent air speed at sea level V_eq divided by surface Regier velocity index V_R as shown in Eq.(4). Regier number R and Flutter number F are inversely proportional and satisfy Eq.(5). The Flutter number corresponding to the equivalent flutter velocity is determined from a set of non dimensional plots as described next and is compared with the actual flutter number in order to determine the flutter velocity safety margin, which should be above 20% at sea level maximum dive speed.

$$\text{Flutter\_number:=}\ V_{Feq}/V\_R = \frac{V_F\sqrt{\sigma}}{0.5C_{75}\omega_\alpha\sqrt{\mu_0}} \tag{4}$$

Hence,

$$\text{Flutter\_number:= Flutter Mach Number / Regier\_no.} \tag{5}$$

INPUT Root and Tip chord: $CR := 35.4 \cdot ft$ $CT := 14.5 \cdot ft$ $\lambda := \frac{CT}{CR}$

INPUT effective SEMISPAN: $Semi\_span := 106.8 \cdot ft$ $\lambda = 0.41$

DefineEffective Aspect ratio: (ONE SIDE ONLY) $AR := \frac{Semi\_span}{0.5 \cdot (CR + CT)}$ $AR = 4.281$

INPUT Torsional Stiffness at effective root, GJ_root and midspan, along and normal to elastic axis:

$GJ\_root := 40 \cdot 10^8 \cdot lb \cdot ft^2$ $GJ\_mid := 24 \cdot 10^8 \cdot lb \cdot ft^2$ $GJ\_Ratio := \frac{GJ\_mid}{GJ\_root}$

INPUT Mach number and Altitude (in 1000 ft): $Mach := 0.6$ $Alt := 0$

INPUT Sweep angle at quarter chord $\Lambda := 37 \cdot deg$

INPUT WEIGHT DATA:

Pitch axis moment of inertia: I_pitch $I\_pitch := 7.0 \cdot 10^5 \cdot lb \cdot ft^2$

Running Pitch moment of inertia at 60% Semi Span: I_60 $I\_60 := 16000 \cdot \left(\frac{lb \cdot ft^2}{ft}\right)$

Running weight at 60% of exposed Span station: W_60 $W\_60 := 500 \cdot \frac{lb}{ft}$

INPUT CG Location at 60% as fraction of MGC chord: CGR $CGR := 0.45$ $MGC := \frac{2}{3} \cdot \left(\frac{1 + \lambda + \lambda^2}{1 + \lambda}\right) \cdot CR$

INPUT Exposed weight per side W_ex $W\_ex := 6.69 \cdot 10^4 \cdot lb$ $MGC = 26.409 \cdot ft$

Fig. 3 Interactive INPUT screen for geometry, stiffness, Mach number, altitude, weight and pitch inertia data.

5 FLUTTER BOUNDARY ESTIMATION

The flutter analysis is accomplished by using two basic normalized flutter index plots, namely Regier number and Flutter number vs. Mach number as shown in Figs. 4 and 5. These plots were based on experimental and analytical flutter studies of these two flutter indexes which were normalized by nominal values of five basic parameters, namely sea level mass ratio, taper ratio, aspect ratio, chord-wise center of gravity position, and pitching radius of gyration. Only those plots applicable to a conventional straight leading and trailing edge plan-form wing with moderate sweep between 20 and 40 degrees, are presented here. The corresponding plots applicable to a conventional plan-form wing with low sweep are presented in Ref 9. High sweep wing and delta wing analyses are included in the latest MathCad and Matlab[10] version. Numerous additional plots are available in the original report[2].

Figure 4 shows the plot of normalized Regier number versus Mach number, for flutter boundary estimation for conventional, moderately swept wings. The upper solid line indicates the upper limits of Regier number versus Mach number for normal values of the key basic parameters (mass ratio = 30, taper ratio = 0.6, aspect ratio = 2 and radius of gyration ratio Rgyb_60 = 0.5). This flutter boundary is a conservative upper limit envelope and is denoted by R_ms_env(M). The

lower dashed line is an average non-conservative limit denoted by R_ms_avr(M). These two plots were compiled[2] by computing the normalized Regier number from numerous experimental data and then drawing an upper bound and a mean line through experimental data points.

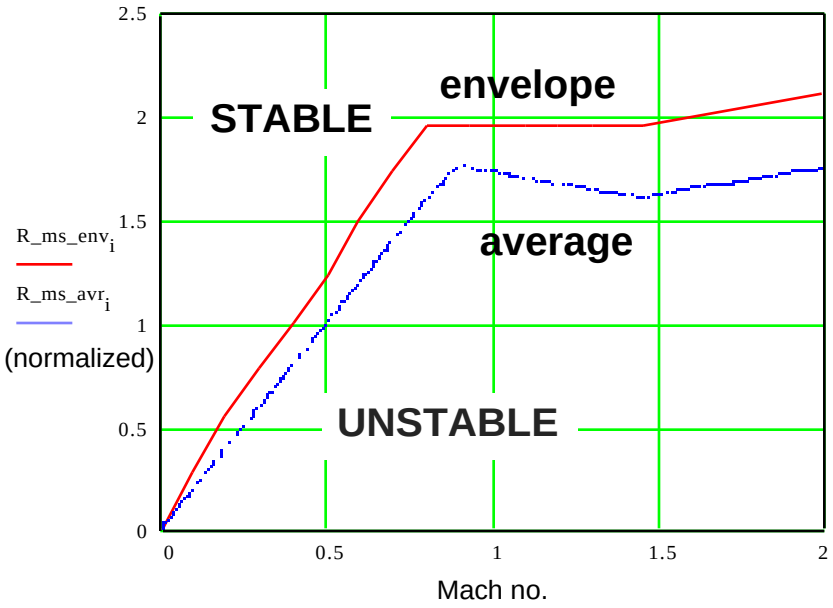

Fig. 4 Normalized Regier no. vs. Mach no. plot for flutter boundary estimation of moderate sweep wings.

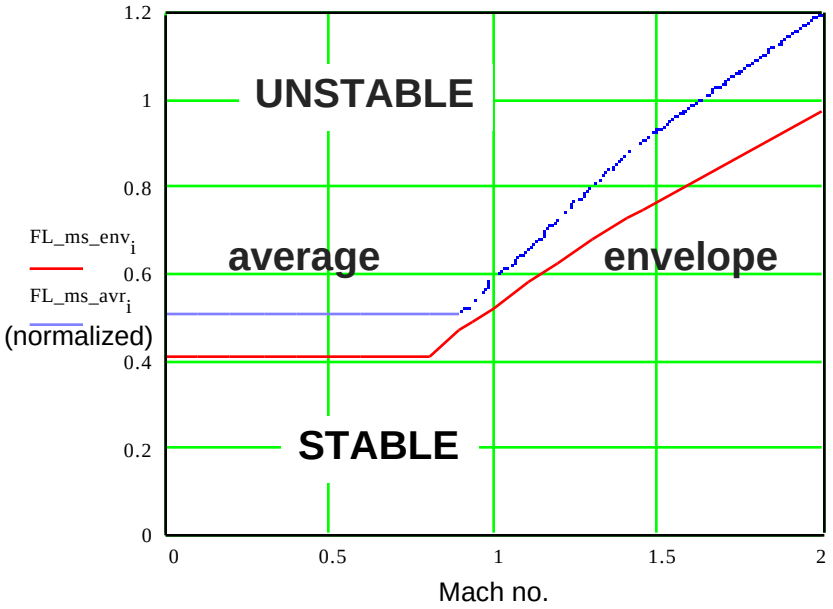

Fig. 5 Normalized Flutter no. vs. Mach no. plot for flutter boundary estimation of moderate sweep wings.

Figure 5 shows the plot of normalized Flutter number versus Mach number for flutter boundary estimation for a conventional moderately swept wing. This plot is also used to estimate the equivalent flutter velocity and flutter dynamic pressure. In this figure the solid line is a conservative lower limit envelope and is denoted by FL_ms_env(M). The dotted line is an average non conservative lower limit flutter boundary and is denoted by FL_ms_avr(M).

Since Figs. 4 and 5 are based on normalized Regier number and Flutter number, the actual Regier number is determined by dividing R_ms_env(M) and R_ms_avr(M) by a total correction factor K_all, to account for actual values of the five key parameters, namely mass ratio $\mu 0$, taper ratio λ, aspect ratio AR, center of gravity ratio CGR and pitch radius of gyration ratio at 60% semispan Rgyb_60 as shown in Eq.6. Since the Flutter number is Mach number over Regier number, the actual Flutter number is determined by multiplying FL_ms_env(M) and FL_ms_avr(M) by the total correction factor K_all as shown in Eq.7. This total correction factor K_all is a product of all five key parameter correction factors for mass ratio k_μm($\mu 0$), taper ratio K_λ, aspect ratio K_Ar(Ar), CG position ratio K_CG(CGR) and radius of gyration ratio K_Rgyb(Rgyb_60) as shown in Eq.8. The relationship between these five key parameters and the corresponding correction factors for moderate sweep wings and plots used to determine these correction factors are presented in Refs.2, 9. This overall correction factor K_all is applied to the normalized stability envelopes R_ms_env(M) and FL_ms_env(M), at the reference Mach number M at sea level, using

$$\text{Regier\_env(M)} := \text{R\_ms\_env(M)} / \text{K\_all} \tag{6}$$

$$\text{Flutter\_env(M)} := \text{FL\_ms\_env(M)} * \text{K\_all} \tag{7}$$

where,

$$\text{K\_all} := \text{K\_}\mu\text{m}(\mu 0)*\text{K\_}\lambda(\lambda)*\text{K\_Ar(Ar)}*\text{K\_CG(CGR)}*\text{K\_Rgyb(Rgyb\_60)}. \tag{8}$$

The overall correction factor K_all is also applied to the normalized average stability bounds R_ms_avr(M) and F_ms_avr(M) in a similar manner. Thus a correction factor greater than unity is beneficial to flutter stability.

Root flexibility Correction Factors: If this effective root is considered to be flexible, additional correction factors Kf_env and Kf_avr are computed and applied to account for the effect of bending and torsional flexibility at this wing station. Additional input required for this correction factor are chordwise location of elastic axis line c_hinge at root chord and the ratio of torsion or pitch frequency over bending or heave frequency fp/fh. The flexibility correction factors Kf_env and Kf_avr are determined using the parametric plots shown in Refs. 2, 9. Then each factor is multiplied by K_all from Eq. (8) and are used to modify the Regier_env(M), Regier_avr(M), Flutter_env(M) and Flutter_avr(M) as shown in Eqs. (6) and (7).

After all the correction factors are applied to the flutter boundary data from Figs. 4 and 5, actual values of Regier_env(M) and Flutter_env(M) are compared with surface Regier number R and Flutter number F of the specific wing under consideration. Suppose, at a given Mach number corresponding to the maximum dive speed at sea level, the computed surface Regier number R and Flutter number F, satisfy the inequalities

$$R > \text{Regier\_env(M)}. \quad \text{and} \quad F < \text{Flutter\_env(M)}, \tag{9}$$

then, the cantilever wing may be considered flutter free at that specified Mach number at sea level. On the other hand, if

$$\text{Regier\_env(M)} > R > \text{Regier\_avr(M)} \quad \text{and} \quad \text{Flutter\_env(M)} < F < \text{Flutter\_avr(M)} \tag{10}$$

then, the wing may be marginally stable or unstable and may require redesign or refined analysis. Finally, if

$$R < \text{Regier\_avr(M)} \quad \text{and} \quad F > \text{Flutter\_avr(M)}, \tag{11}$$

then, the wing has unstable flutter characteristics at the specified Mach number at sea level, and will require redesign.

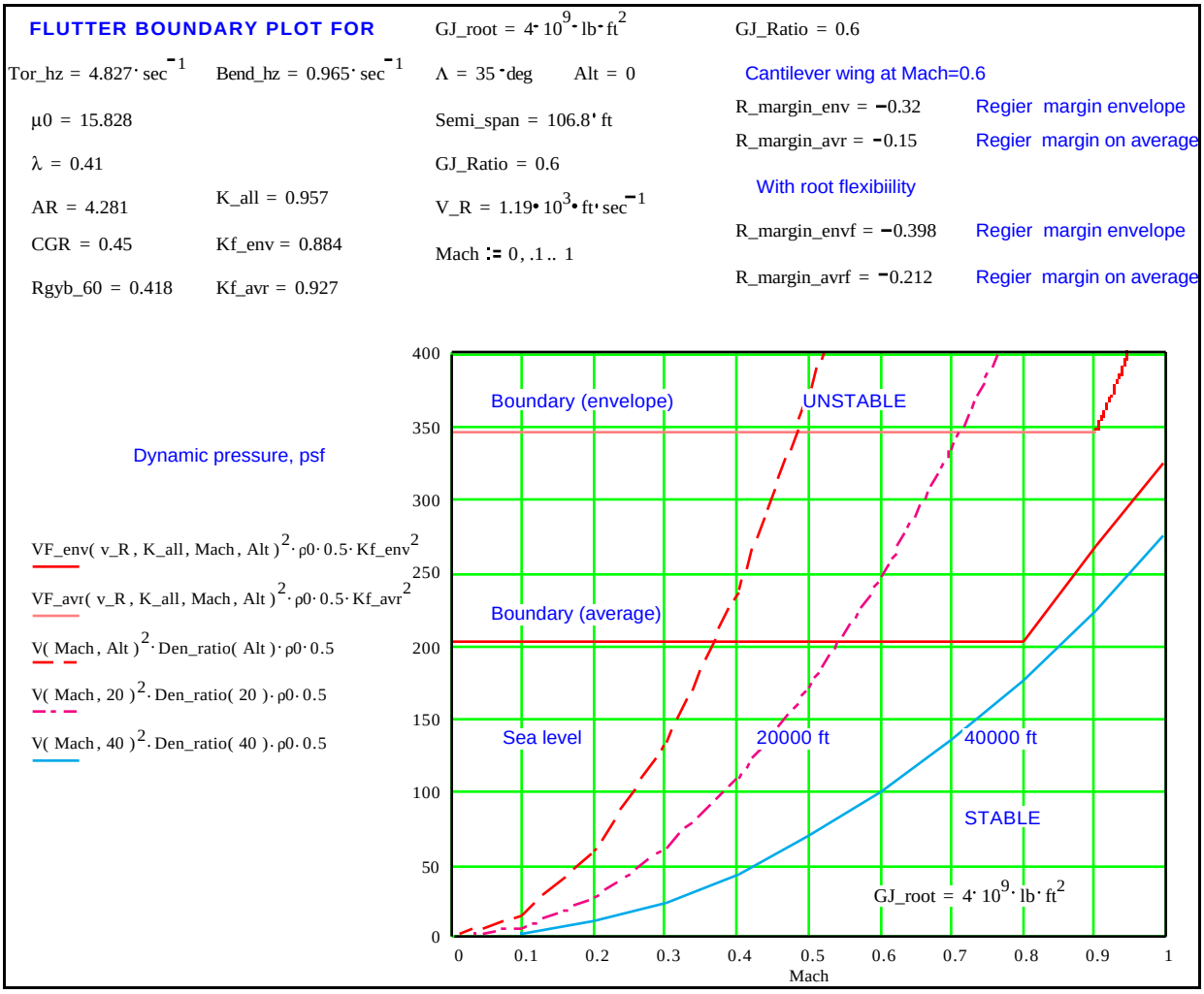

Fig. 6. Summary of interactive flutter analysis results and flutter boundary plot as they appear on the screen.

The surface Regier velocity margins from the upper envelope and average Regier velocity boundary are used to plot the corresponding flutter dynamic pressure boundary. A typical plot of flutter boundary and flight dynamic pressure versus Mach number at sea level, 20000 feet and 40000 feet altitude is shown in Fig. 6, which also shows a summary of all the results along with the flutter boundary plot as they appear in the interactive computer screen. The wing effective root torsion stiffness GJ_root, GJ_Ratio, semi-span, sweep-back angle Λ, primary torsion and

bending frequencies, along with five key parameters μ0, λ, AR, CGR and Rgyb_60 are shown at top and upper left. The corresponding correction factor K_all along with the flexibility correction factors Kf_env and Kf_avr are shown next. The surface Regier velocity *V_R* and surface Regier number margins without and with root flexibility correction at Mach 0.6 are shown at upper right. The sea level flutter velocities VF_env and VF_avr are computed by multiplying the corresponding Flutter_env(M) and Flutter_avr(M) by surface Regier velocity *V_R*.

6 PARAMETRIC STUDY EXAMPLE

Figure 7 shows the baseline outer wing plan-form and value of key parameters of a Blended-Wing-Body aircraft concept[6]. Examples to estimate flutter boundary and outer-wing effective root-chord stiffness requirement are presented. The outer wing has a semi-span of 106.8 feet. The effective root-chord is assumed to have a torsion stiffness of 4×10^9 lb-ft^2. The quarter chord sweep is 37 degrees, the sea level mass ratio is 15.8, the aspect ratio based on the outer wing semi-span is 4.3, the center of gravity line is assumed to be at 45% chord, and the pitch radius of gyration ratio is assumed to be 0.42. Using the empirical method, torsion frequency is estimated to be 4.2 Hz. The results presented here include an effective root flexibility correction factor Kf is Kf_env = 0.88 and Kf_avr = 0.93.

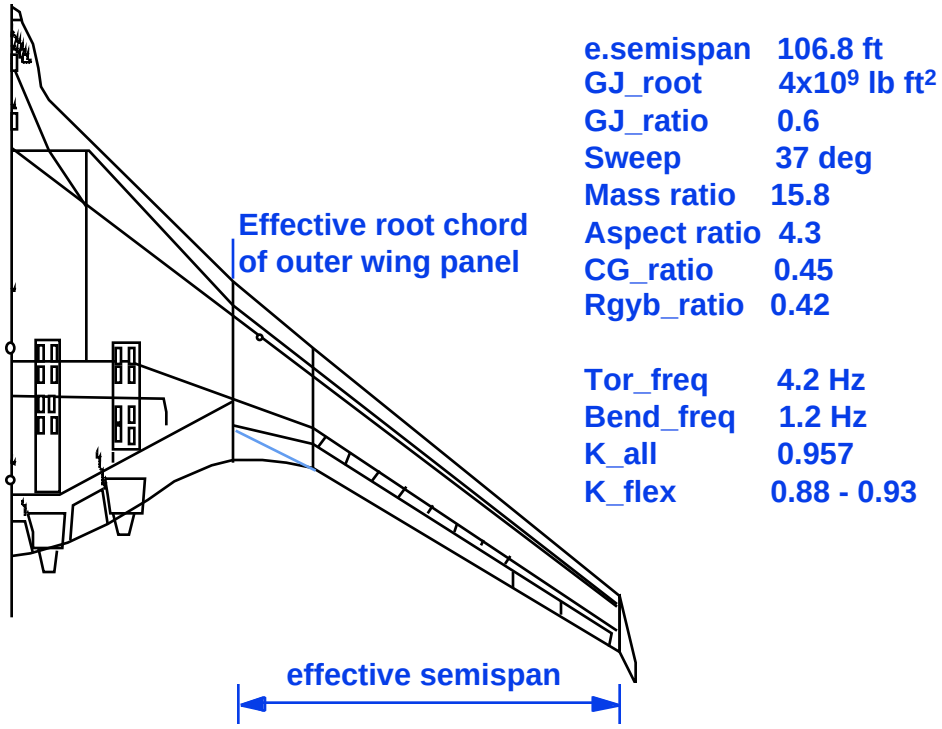

Fig. 7. Data for flutter analysis of the outer wing of a blended wing-body transport concept.

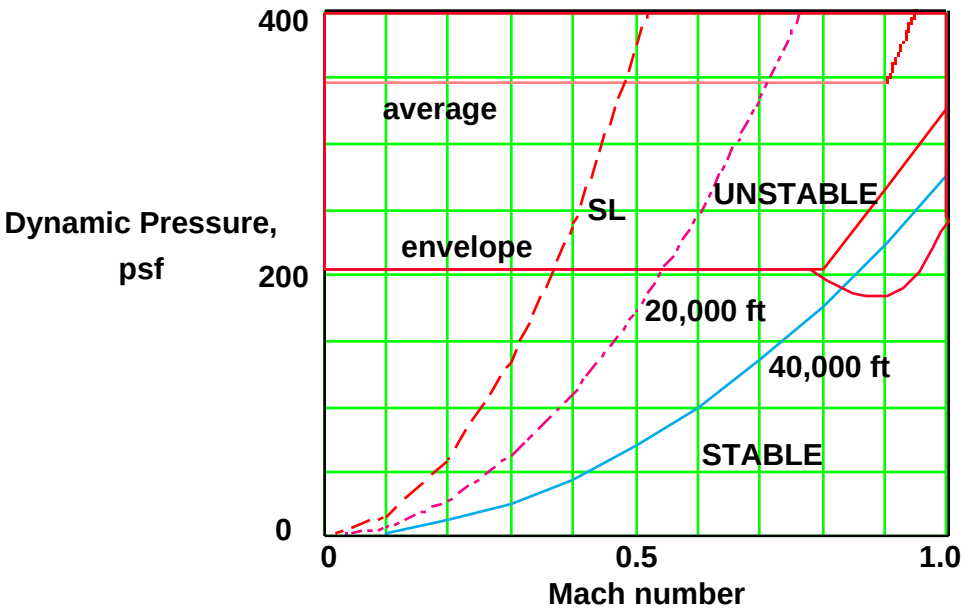

Fig. 8. Outer wing flutter boundary vs. Mach number for wing-root torsion stiffness 40×10^8 lb-ft^2.

Figure 8 shows initial estimates of the outer-wing flutter dynamic pressure boundary versus Mach number for effective root-chord torsion stiffness of 4×10^9 lb-ft^2, at sea level, 20000 feet and 40000 feet altitudes. This figure indicates that the wing would be susceptible to transonic flutter near cruise altitude of 40000 ft and Mach number 0.85. Since the flutter dynamic pressure boundary also has a dip near transonic speed, detailed transonic flutter analysis and wing redesign would be necessary.

Results of a parametric study to estimate adequate torsion stiffness requirement at the outer-wing effective root-chord is shown in Figs. 9 and 10. This exercise demonstrated the versatility and flexibility of this interactive software. First an array of values were assigned to the wing-root stiffness variable GJ_root, while keeping all other geometric parameters fixed. The corresponding Regier numbers and Flutter numbers along with the 'average' and 'envelope' stability boundaries were plotted at the reference Mach number 0.6, at sea level. The corresponding Regier velocity index and flutter velocities were also determined. Fig. 9 shows the variation of Regier number with wing root-chord torsion stiffness and the flutter boundaries at a Mach 0.6, at sea level. The two flutter boundaries labeled 'envelope' and 'average' represent an upper bound and a non-conservative average flutter boundary, respectively. If the Regier number of the wing is greater than the upper boundary of the region labeled 'stable' over the Mach number range, then the wing is considered flutter free. Figure 10 shows the variation of Flutter number with wing root-chord torsion stiffness. If the Flutter number of the wing is smaller than the lower bound of the region labeled 'stable' over the Mach number range, then the wing is flutter free. Figs. 9 and 10 indicate that conservatively, the wing could have 5% to 10% flutter velocity margin at Mach 0.6 at sea level if the wing effective root-chord torsion stiffness exceeded 100×10^8 lb-ft^2.

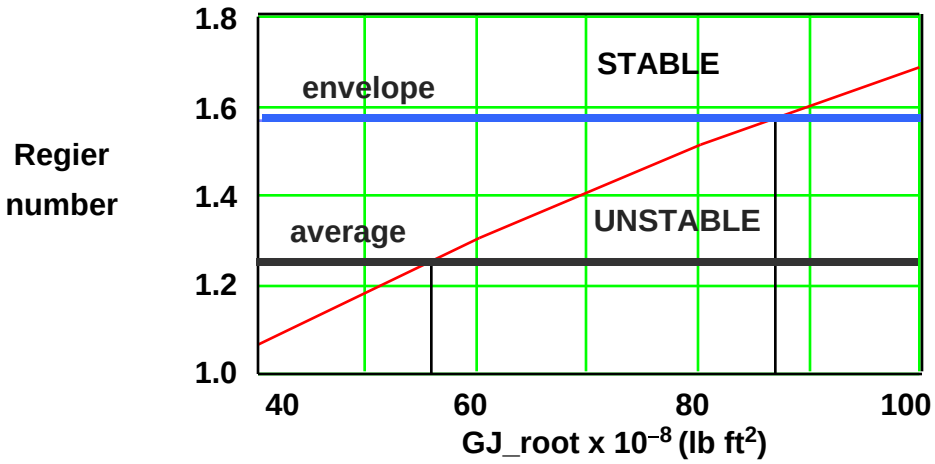

Fig. 9. Variation of surface Regier number with wing root-chord torsion stiffness at a Mach 0.6 at sea level.

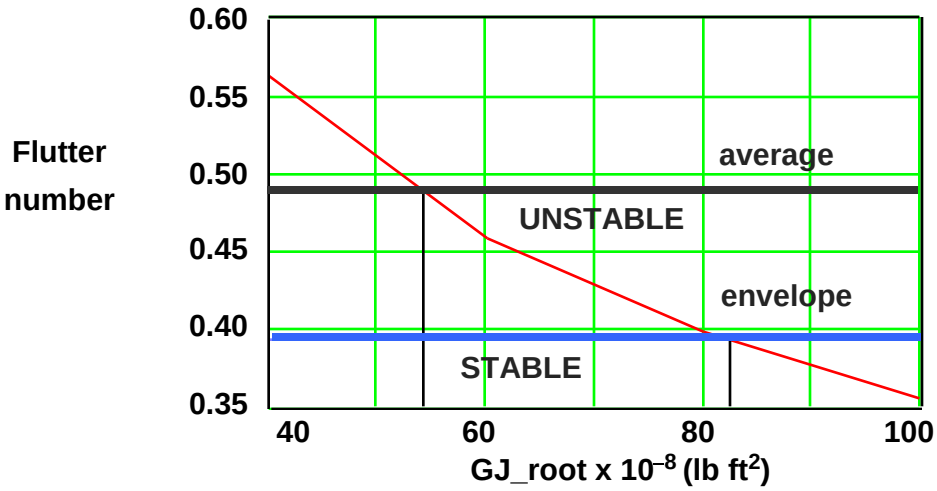

Fig. 10. Plot of Flutter number vs. wing root-chord torsion stiffness at Mach 0.6 at sea level.

7 WING REDESIGN

In these conceptual studies, many of the initial data such as effective wing root torsion stiffness, pitch radius of gyration, and effective wing-root flexibility effects were chosen somewhat arbitrarily and the final results were sensitive to these values. However, the answers provided a good indication of flutter problems and stiffness requirements of such large wings. In a subsequent redesign of this proposed airplane[8] based on flight performance and a new propulsion system, the span of the wing was reduced significantly. In this redesign, the effective semi-span was estimated to be 82.5 ft. Based on the new wing loading and static structural design[8], the torsion stiffness at the effective wing-root chord station was estimated to be 200×10^8 lb-ft^2. The input data and flutter analysis of this redesigned wing with reduced span are presented in Figs. 11 and 12. Some of the preliminary results were originally presented in Ref. 9.

Figure 11 indicates that with this reduced span stiffer wing, the estimated torsion frequency is increased to 6.4 Hz from 4.2 Hz. The ratio of torsion to bending frequency fp/fh is assumed to be 4. Although the radius of gyration has decreased, the increased stiffness, mass ratio and reduced

aspect ratio resulted in a higher overall correction factor and 300% improvement in flutter boundary dynamic pressure.

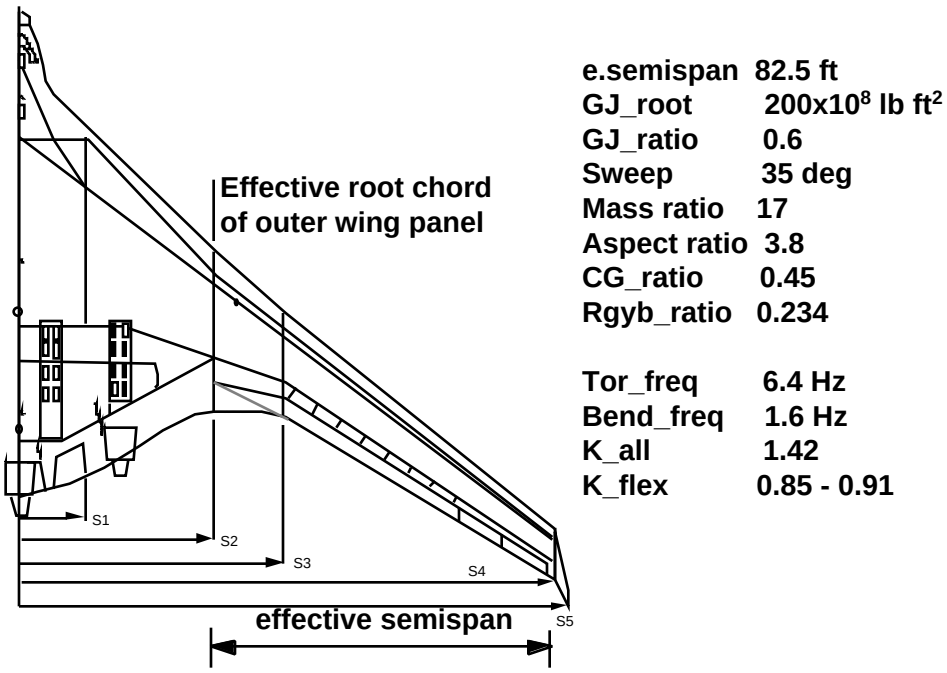

Fig. 11. Geometry and structural data of redesigned wing with reduced span.

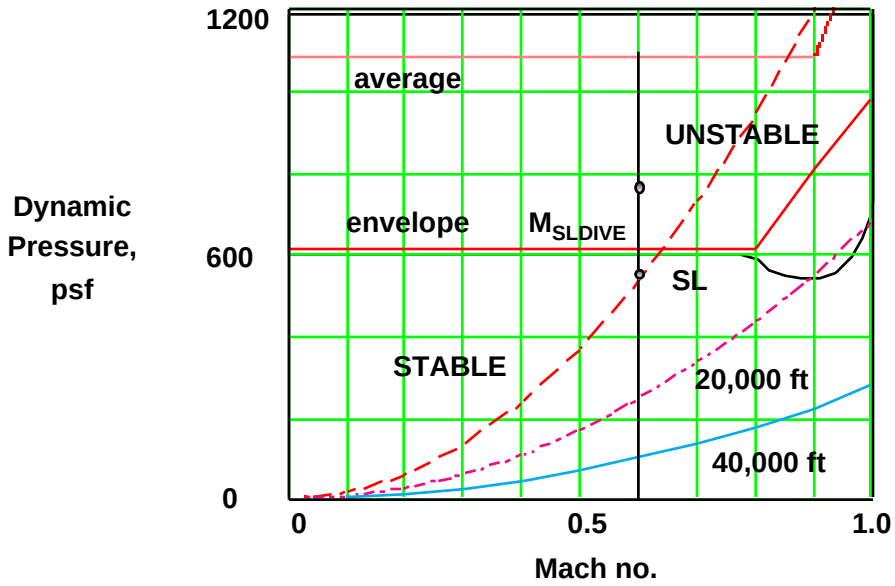

Fig. 12. Reduced span outer wing flutter boundary vs. Mach no. for wing-root torsion stiffness 200x10^8 lb-ft^2.

Figure 12 shows the flutter boundary of the redesigned wing. At sea level the maximum dive dynamic pressure is 550 psf at Mach 0.6, shown by the first dot on the vertical line in Fig. 12. This flight condition falls below the conservative flutter boundary envelope, and can be considered stable. However, in order to maintain a 20% margin in flutter speed or equivalently 44% margin in flutter dynamic pressure, at maximum dive dynamic pressure, the actual flutter

boundary should be above 792 psf, shown by the second dot on this vertical line at Mach 0.6 in Fig. 12. Since the estimated flutter dynamic pressure from the present procedure is between 610 psf and 1080 psf, the main outer wing would marginally satisfy the 44% flutter margin of safety. However, a detailed flutter analysis would be required to complement this conceptual analysis.

8 CONCLUSION

An easy to use, interactive computer program for rapid wing flutter analysis was developed. The analysis was based on non-dimensional parametric plots of Regier number and Flutter number derived from an experimental database and handbook on flutter analysis compiled at Chance-Vought Corporation. Using this empirical method, the effects of wing torsion stiffness, sweep angle, mass ratio, aspect ratio, center of gravity location and pitch inertia radius of gyration could be easily analyzed at the conceptual design stage. An example to investigate flutter characteristics of a wing is presented. An Initial set of flutter instability boundaries and flutter dynamic pressure estimates were obtained. A parametric study estimated the effective wing-root chord minimal torsion stiffness, for a flutter free wing. Due to user interest, an improved Matlab[10] version was developed. Other users[11] improved the MathCad version and developed a Fortran version, and coupled it with an equivalent plate analysis structural code for flutter sizing [12,13].

REFERENCES

[1] MathCad, Version.3.1 Users Guide, MathSoft Inc., 201 Broadway, Cambridge, Mass 02139, 1991. MathCad is registered Trademark of MathSoft, Inc.

[2] Harris, G., "Flutter Criteria for Preliminary Design," LTV Aerospace Corporation., Vought Aeronautics and Missiles Division, Engineering Report 2-53450/3R-467 under Bureau of Naval Weapons Contract NOW 61-1072C, September 1963.

[3] Regier, A. A., "The Use of Scaled Dynamic Models in Several Aerospace Vehicle Studies, "*ASME Colloquium on the Use of Models and Scaling in Simulation of Shock and Vibration*, Philadelphia, PA, November, 1963.

[4] Frueh, F. J., "A Flutter Design Parameter to Supplement the Regier Number," AIAA Journal. Vol. 2, No. 7, July 1964.

[5] Dunn, H. J. and Doggett, R. V. Jr., "The Use of Regier Number in the Structural Design with Flutter Constraints," NASA TM 109128, August 1994.

[6] Liebeck, R, H., Page, M. A., Rawdon, Blaine K., Scott, Paul W., and Wright Robert A., "Concepts for Advanced Subsonic Transports," NASA CR-4628, McDonnell Douglas Corporation, Long Beach, CA, Sep. 1994.

[7] Sweetman, W. and Brown S. F., "Megaplanes, the new 800 passenger Jetliners," *Popular Mechanics*, April 1995, pp. 54-57.

[8] Liebeck, R., H., Page, M. A., "Configuration Control Document CCD-3: Blended Wing Body:" Final report Under Contract NAS1-20275 NASA Langley Research Center, Oct. 1997.

[9] Mukhopadhyay, V., "An Interactive Software for Conceptual Wing Flutter Analysis and Parametric Study," NASA TM 110276, August 1995.

[10] Matlab Reference Guide: "High performance Numerical Computation and Visualization Software," The MathWorks, Inc., Nattick, MA. . Matlab is registered Trademark of MathWorks, Inc.

[11] Private communication, Tibbals, T. F., Sverdrup Technology, Inc. (AEDC Group) Arnold AFB, TN, 2002.

[12] Giles, G, "Equivalent Plate Modeling for Conceptual Design of Aircraft Wing Structure," AIAA Paper 95-3945, Sept. 1995.

[13] Loretti, A. J., III, "Generation of Response Surfaces for Aircraft Structural Wing Weight with Strength and Flutter Sizing," MS Thesis, School of Engg. and Applied Sciences, George Washington University, July 1997.